Journal of Ocean Engineering and Science 10 (2025) 246–257

Contents lists available at ScienceDirect

Journal of Ocean Engineering and Science

journal homepage: www.elsevier.com/locate/joes

An investigation of the dynamic behaviour of two rigid cylinders in a tandem arrangement under vortex-induced vibration

Noor Idora Mohd Sukarnoor[a], Lee Kee Quen[a,*], Aminudin Abu[a], Kang Hooi Siang[b], Noriyuki Kuwano[c], Safari Mat Desa[d]

[a] Intelligent Dynamic and System I-kohza, Malaysia-Japan International Institute of Technology, Universiti Teknologi Malaysia, Malaysia
[b] Marine Technology Center, Faculty of Engineering, Universiti Teknologi Malaysia, Johor Bahru, Malaysia
[c] Kyushu University, Japan
[d] National Hydraulics Research Institute Malaysia (NAHRIM), Selangor, Malaysia

ARTICLE INFO

Article history:
Received 8 March 2022
Revised 25 May 2022
Accepted 30 May 2022
Available online 31 May 2022

Keywords:
Vortex-induced vibration
Rigid cylinders
Tandem arrangement

ABSTRACT

The flow interference of multiple cylinders subjected to vortex-induced vibration (VIV) is a complex response that is not fully understood. This paper investigates the fluid-dynamic behaviour of elastically mounted rigid cylinders where both cylinders were free to oscillate in the cross-flow direction. The cylinders were subjected to uniform water flow at various separation distances of 3.5, 4.0, and 4.5*D* (*D* is the diameter of the cylinder) in a tandem arrangement. Based on the observation, the interference between the cylinders and the unsteady wake from the leading cylinder caused a continuous vibration with no lower branch in amplitude response. While as found in the cases of the single cylinder, there was a lower branch in amplitude response. The results also revealed that the cylinders experienced the VIV and wake-induced vibration (WIV) at each separation distance. Moreover, the leading cylinder oscillated at a larger amplitude at a separation distance of 3.5*D*, indicating a critical distance for cylinders in the tandem arrangement due to the existence of a bistable regime. Hence, it is reasonable to conclude that the flow interference between the leading and trailing cylinders significantly impacts the cylinders' dynamic behaviour.

© 2022 Shanghai Jiaotong University. Published by Elsevier B.V.
This is an open access article under the CC BY license (http://creativecommons.org/licenses/by/4.0/)

1. Introduction

The study of the interaction between the cylindrical structures and current flow towards the vortex-induced vibrations (VIV) has become significant recently. Offshore structures such as cables, pipelines, and marine risers are often exposed to VIV [1,2]. Such structures vibrate when the currents cross them, generating the vortices shed periodically behind them, leading to VIV. This magnitude of vibration could harm the marine riser, for example, when a lock-in or resonance phenomenon is induced [3]. The lock-in phenomenon occurs when the value of vortex shedding frequency matches the natural frequency of the riser [4,5]. When the riser vibrates due to the current flow, vortex streets are formed along its surface, causing an unstable wake region behind the riser. The riser tends to vibrate at large-amplitude oscillations, resulting in stress and fatigue damage [6,7]. The condition worsens when the risers are frequently operated in a group in offshore industries, exposing these structures to strong interaction effects with an unpredictable flow environment [8,9].

In recent years, many attempts have been made to understand the VIV phenomenon. For instance, Kumar and Singh [10] investigated the VIV behaviour of a single bluff body subjected to low subcritical Reynolds number (*Re*). Previous studies such as Fu and Wan [4] and Muddada et al. [5] also conducted numerical works focusing on single cylinder. However, investigations using two cylinders have been limited to date [11]. According to Sumner [12] and Huera-Huarte et al. [13], only a few attentions on the amplitude response have been noticed for a tandem rigid cylinder case. The fluid-dynamic interference of multiple cylinders becomes more complicated than those found on a single cylinder with existing interferences, as it is challenging to gain an in-depth understanding of their dynamic responses [14,15]. Two tandem cylinders can be a benchmark for group arrangement by providing insight into the flow interferences that occur when multiple cylinders are used. Many scholars are still investigating the complicated vibration responses of two tandem cylinders [16–28]. Their studies revealed that complex vibration responses varied due to the

* Corresponding author.
E-mail address: lkquen@utm.my (L.K. Quen).

https://doi.org/10.1016/j.joes.2022.05.035
2468-0133/© 2022 Shanghai Jiaotong University. Published by Elsevier B.V. This is an open access article under the CC BY license (http://creativecommons.org/licenses/by/4.0/)

separation distance (*S/D*) between the cylinders. Furthermore, many researchers acknowledged the significance of *S/D* between cylinders towards the flow interference, formation of vortex and vibration characteristic of a cylinder [27]. The flow interference between the cylinders can be categorised into proximity and wake interferences. The tandem cylinders are subjected to the wake interference as the trailing cylinder is completely submerged in the wake of the leading cylinder.

Several experimental investigations have been conducted on the response of multiple cylinders, where the leading cylinder is stationary and trailing is allowed to oscillate, or both cylinders are stationary. Huang and Sworn [24] previously investigated the hydrodynamic coefficients of two fixed rigid cylinders in a tandem arrangement. In their findings, the shielding effect on the trailing cylinder naturally provided from the leading cylinder influences their mean drag force. However, the shielding effect progressively reduces as the *S/D* between the cylinders increase, causing the drag to increase. Lin et al. [25] reported similar findings for a rigid forced vibration trailing cylinder within a stationary leading wake.

Korkischko and Meneghini [21] assessed the changes in flow dynamics and the galloping phenomenon for multiple rigid cylinders adjacent to one another. Only the trailing cylinder was allowed to oscillate freely. The *S/D* values in this study varied from 2.0 to 6.0. The amplitude response in this study was found interesting, where the amplitude response of the trailing shows a monotonically increased without an upper and lower branch for all *S/D*. The authors claimed that the response of the cylinder was observed as wake-interference vibrations (WIV). Accordingly, similar results have also been obtained by Assi et al. [19] who performed an experiment of rigid cylinders in tandem with only the trailing cylinder was free to oscillate.

On the other hand, Kim et al. [20] assessed the interaction between two tandem cylinders in a wind tunnel with an *S/D* of 1.1 to 4.2, where *S* denotes the gap between the two cylinders and *D* denotes the diameter of the cylinder. The study examined three distinct experimental conditions, namely, allowing two of the cylinders to oscillate freely, allowing only the trailing cylinder to oscillate, and allowing only the leading cylinder to oscillate. Furthermore, it reported five regimes that described the vibration behaviour, based on the *S/D* between the cylinders. In the first (*S/D* was larger than 0.1) and fourth regimes (*S/D* was larger than 2.0), the cylinder vibrations were negligibly smaller, whereas, in the second regime, the cylinder vibrations were violent. The leading cylinder oscillated almost independently of the trailing cylinder. While the trailing cylinder remained fixed in the third regime, the leading cylinder was found to vibrate slowly. In the fifth regime (*S/D* was larger than 2.7), where the *S/D* between the cylinders was farthest, the cylinders behaved identically to a single cylinder. Meanwhile, Bokaian and Geoola [29] proposed four types of vibrations when allowing only the trailing cylinder to oscillate transversely in a uniform flow. Depending on the *S/D*, the galloping, vortex excitation and separated vortex excitation and galloping were observed. Moreover, the authors also identified the combination of vortex excitation and galloping phenomena. The numerical simulation by Fan et al. [30] also demonstrated similar results. The authors used large eddy simulation (LES) and rigid body numerical simulation to study the vibration mode of three tandem cylinders. Additionally, Huera-Huarte and Bearman [22] discovered different regimes in their study using two flexible cylinders at a distance of 2.0 to 4.0 with Reynolds number (*Re*) up to 12,000 in a water flume. According to the authors, different types of oscillations between the cylinders were identified, namely VIV, WIV, and a combination of the two. The response of WIV is achieved when the cylinder's amplitude increases as the reduced velocity increases. This oscillation amplitude is constantly increasing as a result of the turbulence produced by the leading cylinder. Thus, the distance between the cylinders affects the formation of the WIV [31].

Meanwhile, in the case of flexible cylinders, Huera-Huarte and Gharib [23] extended the research of Huera-Huarte and Bearman [22] by utilising a larger *S/D* range of 4.0 to 8.0 and reported that the leading flexible cylinder exhibited single cylinder's behaviour at such large *S/D*. Similarly, Xu et al. [27] reported similar findings using two flexible cylinders in a tandem arrangement with a large *S/D* of 4.0 to 16.0. Furthermore, Wang et al. [31] added that the leading flexible cylinder responded as a single cylinder with the characteristics of a common VIV response when the cylinders were installed far apart.

Several researchers have investigated the flow interference between the cylinders through numerical technique, however the case studies were at a very low *Re*. Zhao et al. [32] conducted a simulation study to examine the VIV of two rigid cylinders in a tandem arrangement with *S/D* values ranging from 0.5 to 3.0. The results indicated that the amplitude of responses for both cylinders vibrated more significantly than a single cylinder for all cases of *S/D*. Similarly, Mysa et al. [33] revealed a vibrating behaviour of two tandem cylinders at low *Re* numerically with an *S/D* of 5.0. According to the authors, turbulence produced by the leading and trailing cylinders significantly contributed to the coupled responses in the tandem arrangement. It included an increased CF load and oscillations generated by the trailing cylinder in the post lock-in region. Meanwhile, Singh et al. [34] focused on the two-cylinder wake interference at different angular positions of leading cylinder (α = 0°, 30°, 45°, 60°, 90°), which resulting the cylinders to be in tandem and side-by-side arrangement at a fixed S/D = 3.0. It was reported that the hydrodynamic forces for both cylinders were increased with an increased in the angular position for the leading cylinder, except for the lift coefficients for the trailing cylinder.

On the other hand, Zdravkovich and Pridden [17] highlighted the existence of a critical separation distance for multiple cylinders where the gap pressure coefficient was greater than the base pressure value. The cylinders could vibrate more significantly during the critical *S/D* and worsen the damage of the cylinder. The data on the critical *S/D* for tandem cylinders is still unclear and would be useful to discover for different experimental conditions. Sharman et al. [35] studied the behaviour of two fixed tandem cylinders numerically and reported an unusual increment in fluctuating forces and the Strouhal number (*St*) at the critical *S/D*, which was found between 3.75 and 4.0*D*. Whereas, Korkischko and Meneghini [21] reported that, the critical *S/D* of 3.0 resulted in a large amplitude oscillation of the trailing cylinder. In contrast, Mysa et al. [33] discovered that the critical distance to be between 3.5 and 5.0*D*.

Although previous literature yielded excellent findings involving multiple cylinders, further assessments are required to gain a better understanding. Hence, the present study highlighted two main gaps. Firstly, there is a dearth of experimental evidence for the VIV using two elastically mounted rigid cylinders. The VIV characteristics become more complicated when both cylinders can vibrate. Since previous research on the leading cylinder has primarily been conducted in a stationary state, the present study will explore the cylinders' responses when both cylinders are allowed to vibrate. In a real application, the VIV phenomenon may become more violent and complicated when an oscillating leading cylinder is involved [35].

Secondly, the data on dynamic responses of a single degree of freedom is still limited, as previous literature has mostly focused on either leading or trailing cylinder's behaviour. Whereby, a detailed comparison of both cylinders' behaviour is still scarce. Only a few studies have discussed the behaviour of both cylinders to understand the VIV of two oscillating cylinders in tandem arrangement. However, in previous studies, either the leading cylinder was

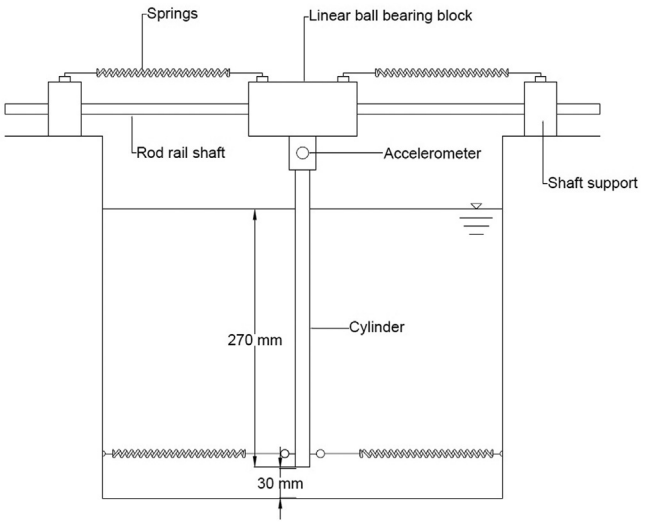

Fig. 1. Experimental setup.

fixed while the trailing cylinder was allowed to vibrate, or both cylinders were fixed. There are no published studies to present the results of rigid cylinders allowed to vibrate in a CF direction. Since most of the risers in offshore industries are not in a fixed condition, investigating the VIV of the oscillating cylinders is feasible. This present study discusses the effects of *S/D* on the VIV through the amplitude and frequency responses of the cylinders, where the *S/D* was set from 3.5 to 4.5 (the critical distance range was based on literature). The VIV study emphasises the critical *S/D* for multiple cylinders in a tandem arrangement, as they are of interest to discover.

This paper is divided into five sections, including this section. Section 2 addresses the experimental arrangement of this study. Section 3 discusses the validation of the experiments through the cases of a single cylinder and two cylinders. Section 4 presents cylinders' experimental results in a tandem arrangement. Finally, Section 5 concludes the experimental findings and includes potential future work.

2. Materials and methods

A water flume with length of 50.0 m, height of 0.70 m, and width of 0.75 m was utilised to conduct the experiment. The designed water level was maintained at 0.3 m. The water flume pump generated a uniform flow rate of 0.1 to 0.6 m/s at an interval of 0.03 m/s, resulting the Reynolds number, *Re* ranged from 3120 to 31,200. While the turbulence intensity (*Ti*) was around 1.9% at an inflow velocity of 0.3 m/s.

Hollow polyvinyl chloride (PVC) cylinder models were chosen in this experiment. The models, vertically mounted (Fig. 1) in the test section, had a submerged length (L) of 270 mm and a diameter (D) of 25 mm.

The cylinder with an aspect ratio (L/D) of 10.8 was constantly utilised. The cylinder mass ratio (m^*) is 1.5, as calculated by the equation of 4 m $/\pi \rho D^2 L$, where m is the total mass of a cylinder and ρ is the fluid density. The mass ratio obtained in this present study was within the range of riser pipes in marine engineering [11]. The structural damping coefficient in air (ζ) of 0.0954 led to a mass-damping parameter ($m^*\zeta$) of 0.1431. The main properties of the rigid cylinder model are listed in Table 1.

The model was installed as depicted in Fig. 2(a) with a spacing of 30 mm above the flume bottom. Four springs were mounted symmetrically at both ends of each model. The model's design was adopted based on a previous study [36]. The cylinder's upper part

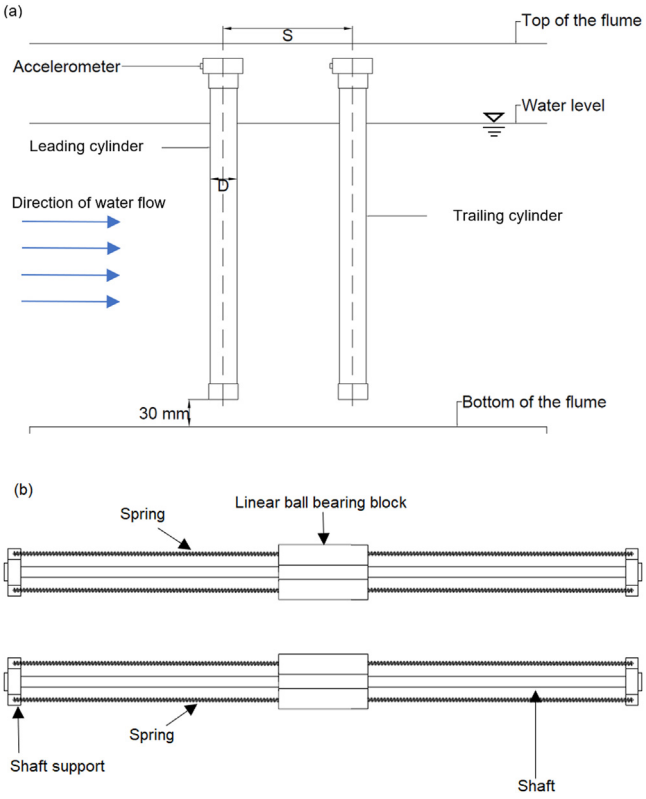

Fig. 2. Two tandem cylinders in a uniform flow (a) side view and (b) top view.

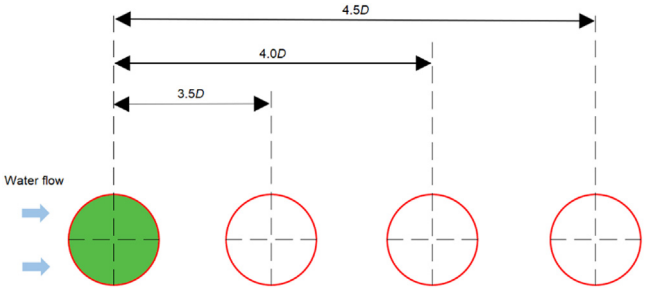

Fig. 3. Two rigid cylinders in a tandem arrangement at various separation distances.

was attached to a linear motion ball bearing block with a shaft to restrict motion only in the cross-flow, CF direction (Fig. 2(b)). The separation distance, *S/D* was set to 3.5, 4.0, and 4.5 as shown in Fig. 3. The displacement and frequency responses of the cylinders were recorded using the triaxial accelerometers (Dytran) with a sensitivity of 10.02 mV/g that were attached to the cylinder's upper part.

3. Validation of experiment

In this subsection, the results for a single circular cylinder are presented for validation purposes.

The amplitude response ratio of a single cylinder was calculated based on the average amplitude value of 10% of the highest peak amplitude, A_y, divided by the cylinder's diameter, D. The same technique was employed by Korkischko and Meneghini [21] and Franzini et al. [37]. Meanwhile, the reduced velocity (V_r) was calculated as follows:

$$V_r = \frac{U}{f_n D} \tag{1}$$

Table 1
Main parameters of the cylinder model.

Parameters	Values
Total length (l)	580 mm
Submerged length (L)	270 mm
Outer diameter (D)	25 mm
Inner diameter (d)	23 mm
Aspect ratio (L/D)	10.8
Spring stiffness (k)	26.93 N/m
Total mass of a cylinder, including a ball bearing block and a shaft (m)	0.199 kg
Mass ratio (m^*)	1.5
Mass-damping ($m^*\zeta$)	0.1431

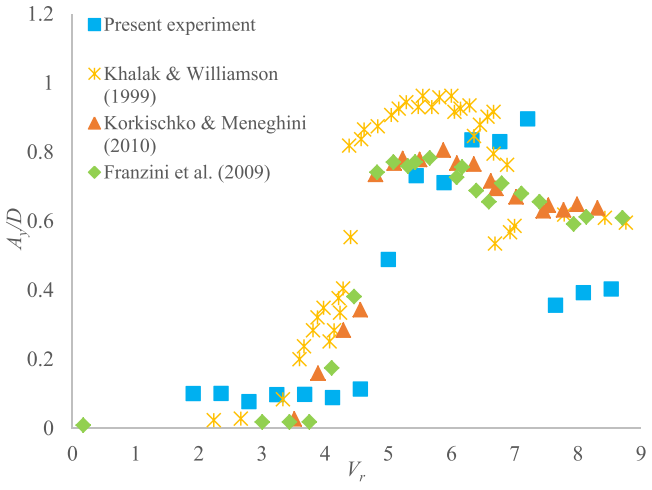

(a)

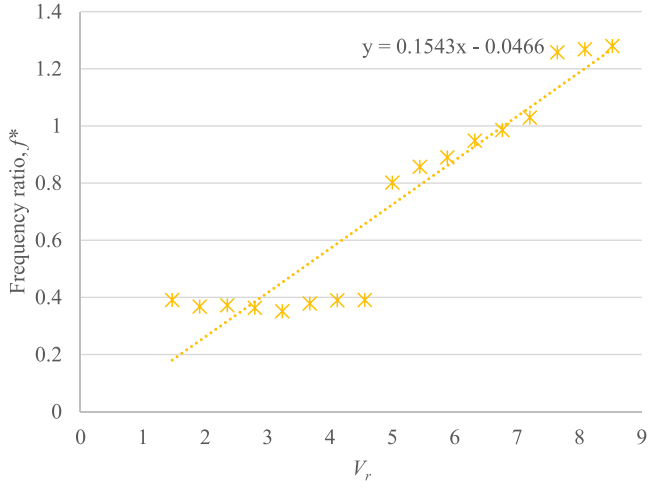

(b)

Fig. 4. Comparisons of the single cylinder's dynamic responses (a) Amplitude response, and (b) frequency response.

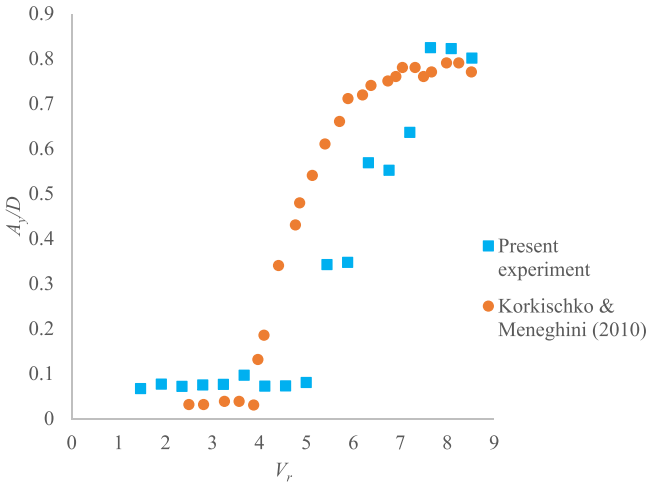

Fig. 5. A comparison of trailing cylinder's amplitude response in a tandem arrangement at separation distance of 4.0D.

where U is the water velocity and f_n is the cylinder's natural frequency. The natural frequency in this experiment was 2.72 Hz, as obtained from the free decay test in still water.

Fig. 4(a) illustrates the amplitude responses of the present study and previous studies [21,37,38]. Three common branches of amplitude responses, referred to as the initial, upper, and lower branches (Fig. 4(a)), were observed in all cases. According to Martin and Avila [39], the three typical amplitude branches existed in a low mass system. The lock-in region formed as V_r increased from 5.0 to 7.2, where the vibration frequency (f) was similar or close to the natural frequency (f_n) (Fig. 4(b)) [39–41]. The lock-in region occurred within the normal range as previously reported, which was less than 8.0 [41]. However, in the present study, the lock-in phenomenon was slower than in the other three studies due to the high damping of the experimental rig [39,42,43]. Because of the occurrence of the slower lock-in region, the lock-out was also deferred to $V_r \approx 7.6$. At approximately $V_r = 7.2$, the amplitude response reached its peak value of 0.89 in the upper branch, while the amplitude value dropped within the lock-out region.

The amplitude response was consistent with the frequency response, which showed a drop in amplitude due to the lock-out phenomenon, $7.6 \leq V_r \leq 8.5$. In the lock-out region, the frequency ratio did not remain close to 1. Meanwhile, Fig. 4(b) indicated that the Strouhal number, St obtained in this experiment was 0.1543. The St value obtained in this study was similar to that obtained by Rahman and Thiagarajan [44] for the cylinder with a low aspect ratio. During the lock-in region at the upper branch, the frequency ratio for the VIV in water was slightly greater than 1 due to the added mass effect [45]. Additionally, the cylinder's frequency response pattern during the lock-in region resembled Khalak and Williamson's [38] description of the cylinder's frequency response in water. This present study's frequency response emphasised the characteristic of the VIV phenomenon for a low mass cylinder in water. As a result of this frequency response, it was possible to define a cylinder with a low mass ratio as having a nonclassical lock-in phenomenon because the frequency ratio was not exactly equal to unity during the lock-in region.

Besides the single cylinder, the present study compared the trailing cylinder's amplitude response in a tandem arrangement to a previous study for validation purposes. Fig. 5 shows a comparison of the trailing cylinder's amplitude response in the present

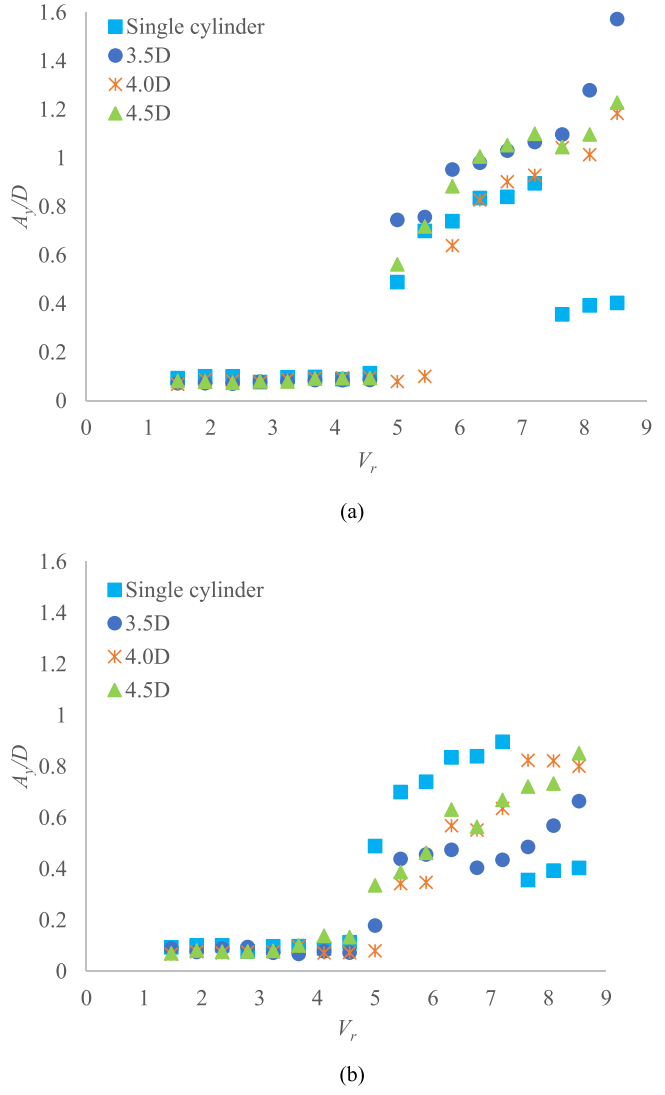

Fig. 6. Graphs comparing the amplitude responses of the (a) leading and (b) trailing cylinders in tandem arrangement to the amplitude response of a single cylinder.

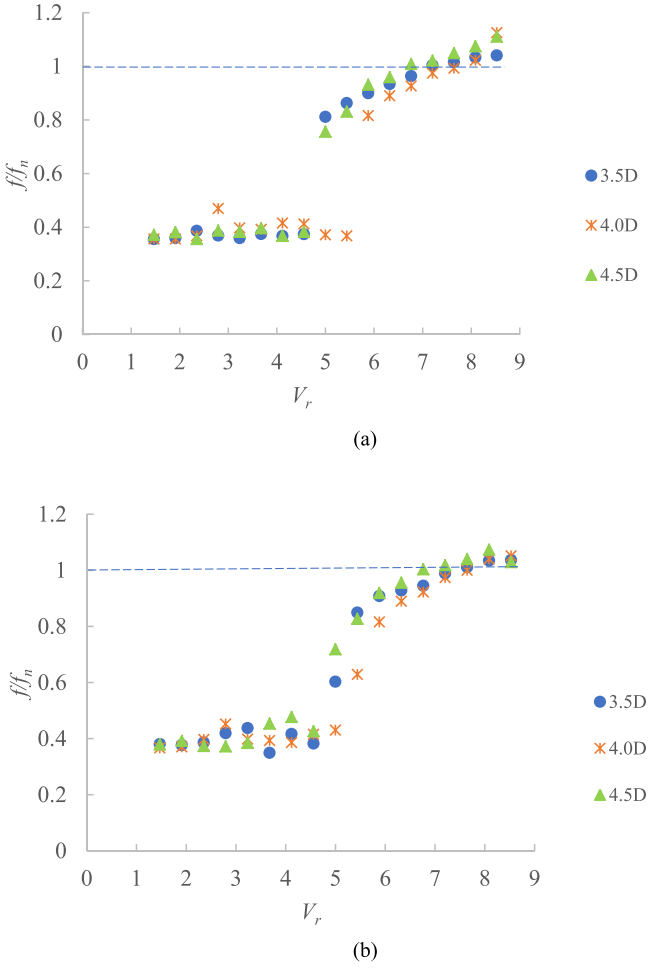

Fig. 7. Frequency responses of (a) leading and (b) trailing cylinders at different *S/D*.

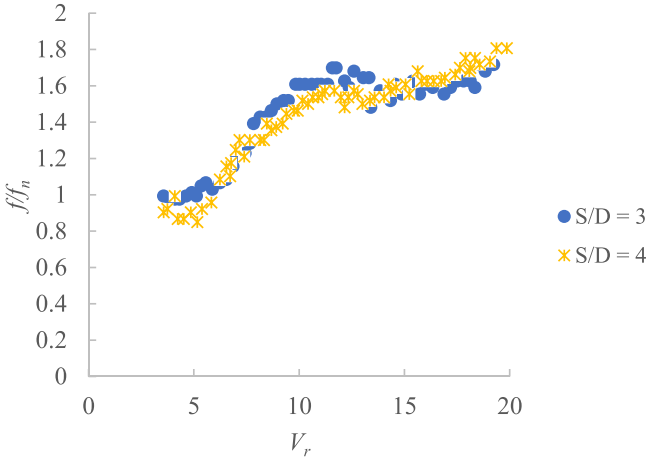

Fig. 8. Frequency responses of trailing cylinder at 3.0*D* and 4.0*D*, by Korkischko and Meneghini [21].

study to that of Korkischko and Meneghini [21]. Korkischko and Meneghini's [21] study omitted discussion of the leading cylinder's response due to the fixed condition of their leading cylinder. Therefore, no further comparisons to the present study are possible. Due to the variable's limitation on separation distances, only $S/D = 4.0$ is shown in Fig. 5. It was observed that, as the reduced velocity increased, the trailing cylinder's amplitude response in the present study became almost comparable to their response. Both amplitude responses were devoid of the lower branch as the oscillation amplitude increased to a higher reduced velocity. Korkischko and Meneghini [21] obtained a slightly earlier lock-in region than this study, which could be explained by the lower mass-damping of their structure. Hence, it can be concluded that their oscillation amplitude behaviour was consistent with that observed in the present study

4. Results and discussion

4.1. Amplitude response of the cylinders in tandem

This section discusses the CF vibration response of two rigid cylinders. The amplitude ratio of the cylinder (A_y/D) was calculated as mentioned in Section 3. The behaviour of two elastically mounted cylinders in a tandem arrangement towards theww flow interference was examined at *S/D* of 3.5, 4.0, and 4.5. At each *S/D*, the amplitude responses for both leading and trailing cylinders are presented in Fig. 6(a) and Fig. 6(b), respectively. Besides, the figures include the oscillation amplitude of the single cylinder as a reference.

The leading cylinder's response characteristics demonstrated a continuous increase as the reduced velocity increased, for all sep-

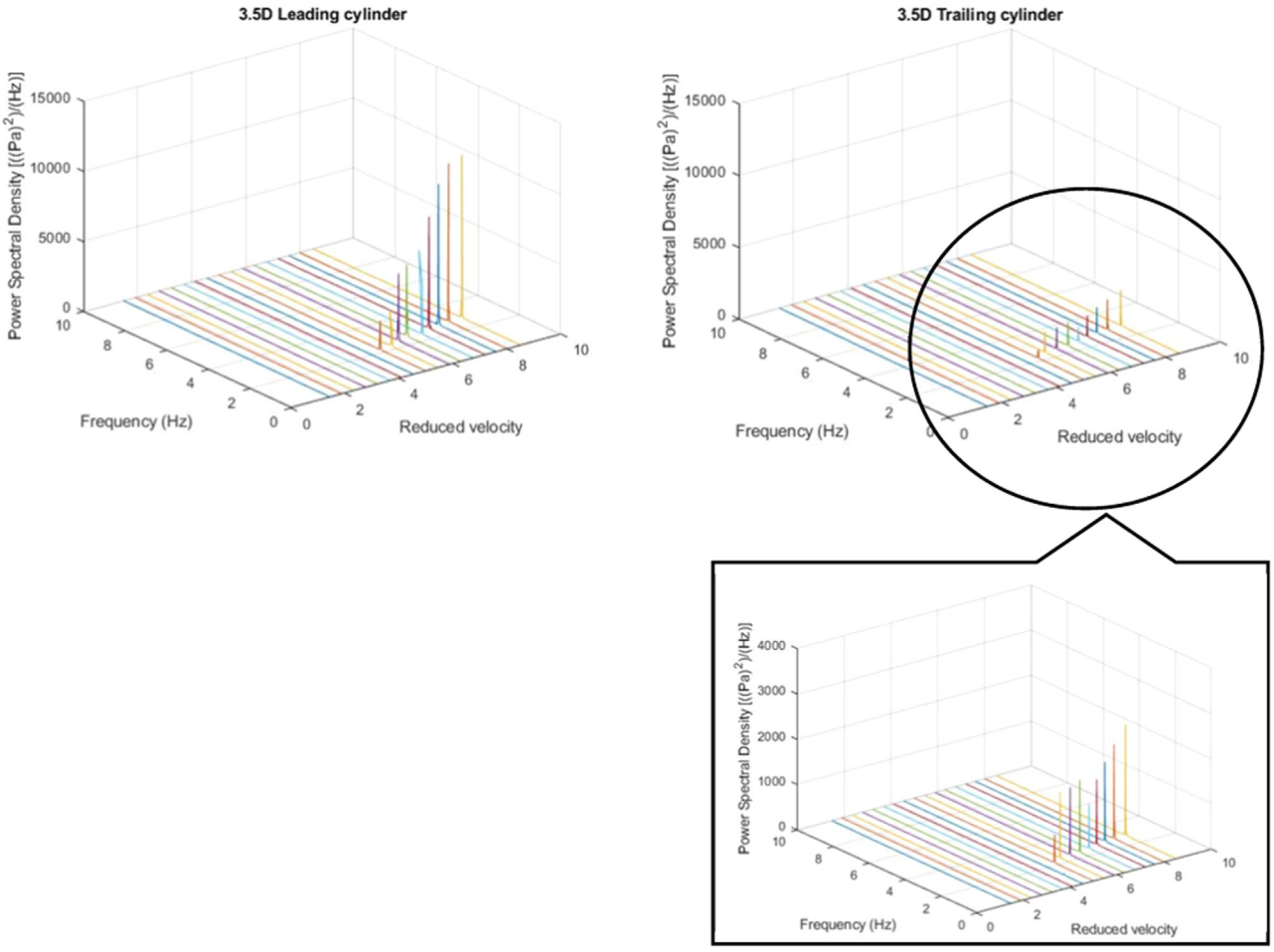

Fig. 9. PSD graphs of bare cylinders in tandem at 3.5*D*.

aration distances (Fig. 6(a)). Whereas, Fig. 6(b) depicts the trailing cylinder's amplitude following the trends of the leading cylinder (Fig. 6(a)), without the presence of a lower branch that was usually present in an oscillating single cylinder. It was suspected that this excitation in amplitude response was due to the wake-induced vibration (WIV), which both cylinders experienced for all tested *S/D*. It was well established that WIV most frequently happened when two or more cylinders were present in a flow, where their wakes could interfere. The formation of vortex shedding in the separation region between the cylinders and the vortex behind the trailing cylinder led to the emergence of WIV [19]. The unsteady wake generated by the leading cylinder caused both cylinders to vibrate, and the cylinders were excited to oscillate at high amplitudes up to the maximum tested V_r [19,41,46]. The findings were similar to those of several previous studies [19,21,26,47], where the scholars investigated the vibration of two tandem cylinders. As anticipated, the result was completely contradictory to that obtained with the single cylinder. Furthermore, this finding proved that the presence of multiple cylinders in a flow could result in a drastic change and worsen the structure's vibration when compared to the single cylinder [48]. The single cylinder's maximum amplitude was determined to be 0.89*D*, which was significantly less than the leading cylinder's maximum amplitude at all separation distances. However, in order to confirm the emergence of WIV in this present study, it was suggested that the experiment be performed with a higher reduced velocity in the future study, which will necessitate the use of a powerful water pump.

On the other hand, the graph plotted for the multiple cylinders indicated that the cylinders were sensitive to the separation distance. Both cylinders began to vibrate at $V_r = 5.0$ and the vibration continued to intensify as V_r increased to 8.5. Based on Fig. 6(a), the leading cylinder experienced a critical condition of vibration because its oscillation amplitude was higher than that of the trailing cylinder at all *S/D*. It was due to the fact that in the tandem arrangement, the leading cylinder provided a shielding effect for the trailing cylinder, preventing the trailing cylinder from vibrating excessively.

At a separation distance of 3.5*D*, the arrangement of the leading cylinder was closest to the trailing cylinder. Based on Fig. 6(a), the leading cylinder's highest amplitude response was $A_y/D = 1.57$, which was amplified by about 292.0%, when compared to the single cylinder's oscillation at $V_r = 8.5$. On the other hand, 195.0% and 207.5% of amplitude amplification were observed for the leading cylinder at $S/D = 4.0$ and 4.5, respectively at $V_r = 8.5$. Thus, the critical separation distance of 3.5*D* was selected for these two-cylinder arrangements due to the high oscillation amplitudes recorded by the leading cylinder at 1.57*D*. According to Zdravkovich [49], this condition was due to the existence of a bistable regime at this separation distance. Based on Huera-Huarte and Bearman [22] and Zdravkovich [49], the bistable regime emerges between 3.0 and 3.8*D*. The regime has been described as having an intermittent appearance of two flow patterns, with the flow transitioning between the vortex formation from the leading cylinder and the reattachment [18,49,50]. This flip-flopping or switching

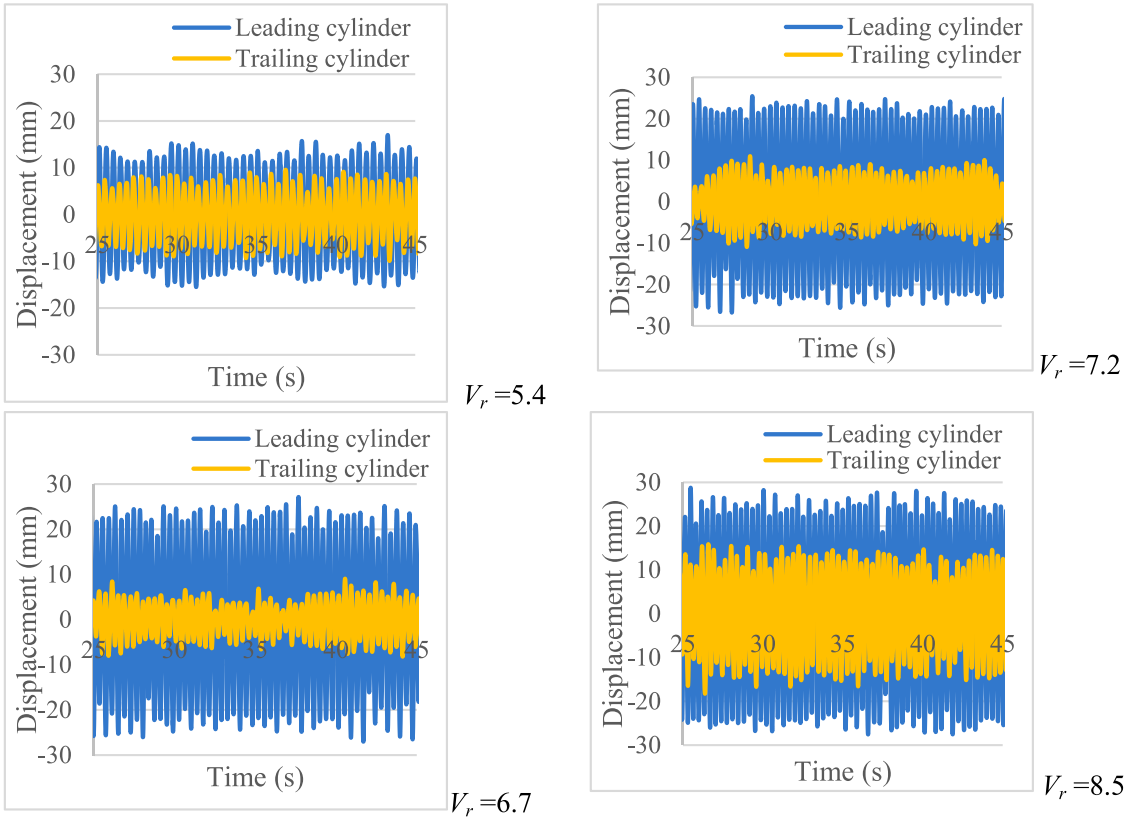

Fig. 10. The oscillation amplitudes of leading and trailing cylinders at 3.5*D*.

phenomenon intermittently changed repeatedly, and this sudden change in the flow excited a large amplitude of oscillation on the leading cylinder [18,50,51]. Meanwhile, Ishigai et al. [52] who discovered 3.8*D* as the critical distance in their study also added that a discontinuous 'jump' in the base pressures at the critical distance increased the cylinder's amplitude.

For the leading cylinder at $S/D = 4.0$ and 4.5, which was greater than a critical spacing, the leading cylinder's oscillation amplitudes increased as the reduced velocity increased. The large oscillations for both cylinders were due to the presence of WIV for wider *S/D*, which was caused by the generated vortex shedding from the leading cylinder [23]. The leading cylinder oscillated at 4.5*D* with large amplitude, almost identical to the response at 3.5*D* up to $V_r = 8.5$. The excitation of the leading cylinder at 4.5*D* was due to the strong effect of WIV generated by the formation of a large vorticity in the gap region.

At a separation distance of 3.5*D*, during the intermittent reattachment of the boundary layer generated by the oscillating trailing cylinder to the boundary layer by the leading cylinder, no shedding was produced from the leading cylinder. This boundary layer attachment caused vortices to be generated behind the trailing cylinder. The interaction between the cylinders was controlled by the leading cylinder and therefore, the trailing cylinder's movement at 3.5*D* was disrupted, resulting in reduced motion [22]. In other words, the turbulence generated by the leading cylinder modified the flows towards the trailing cylinder, as the trailing cylinder was in the wake of the leading cylinder. This flow modification would disturb the wake dynamics and the vortex formation region of the leading cylinder [53]. The boundary layer reattachment was the reason why the trailing cylinder at 3.5*D* exhibited a smaller amplitude response than at other separation distances (4.0*D* and 4.5*D*). Huera-Huarte and Bearman [22] previously confirmed this finding, which was also supported by Zheng et al. [54].

According to Zdravkovich [49], during the co-shedding regime where *S/D* was larger than 3.8, the motion of trailing cylinder was influenced by the leading cylinder's vortex shedding. The vortex shedding was discovered almost between the cylinders throughout the experiment. When the leading cylinder was sufficiently separated from the trailing cylinder, the leading cylinder's vortices collided with the trailing cylinder and merged with the trailing cylinder's vortices. As mentioned before, the shedding from the leading cylinder was unable to excite the trailing cylinder, but this impingement of vortices shed from the leading cylinder onto the trailing cylinder forced the trailing cylinder at 4.0*D* and 4.5*D* to vibrate more vigorously than at 3.5*D*. Based on Fig. 6(b), the trailing cylinder suffered a critical oscillation at a distance of 4.5*D*. The trailing cylinder's amplitude response at 4.5*D* was nearly identical to the amplitude response at 4.0*D* due to the small difference in the value of the selected separation distance. The trailing cylinder vibrated excessively at 4.5*D* compared to other separation distances due to the complex interaction between the large vortices from the leading cylinder and the Kàrmàn vortex street in the gap region.

4.2. Frequency response

Fig. 7 represents the frequency response of the multiple cylinders at various separation distances. The vibration frequency in the CF direction over the natural frequency for both cylinders increased along with V_r. The slow jump of the leading cylinder's frequency response at 4.0*D* in Fig. 7(a) caused a lower amplitude response in that *S/D*. Meanwhile, the frequencies of the leading and trailing cylinders at 3.5 and 4.5*D* started to lock-in at $V_r = 5.0$.

The frequency of the leading cylinder continued to increase monotonically and eventually separated from the natural frequency at $V_r = 8.5$ for all separation distances. The leading cylinder's oscil-

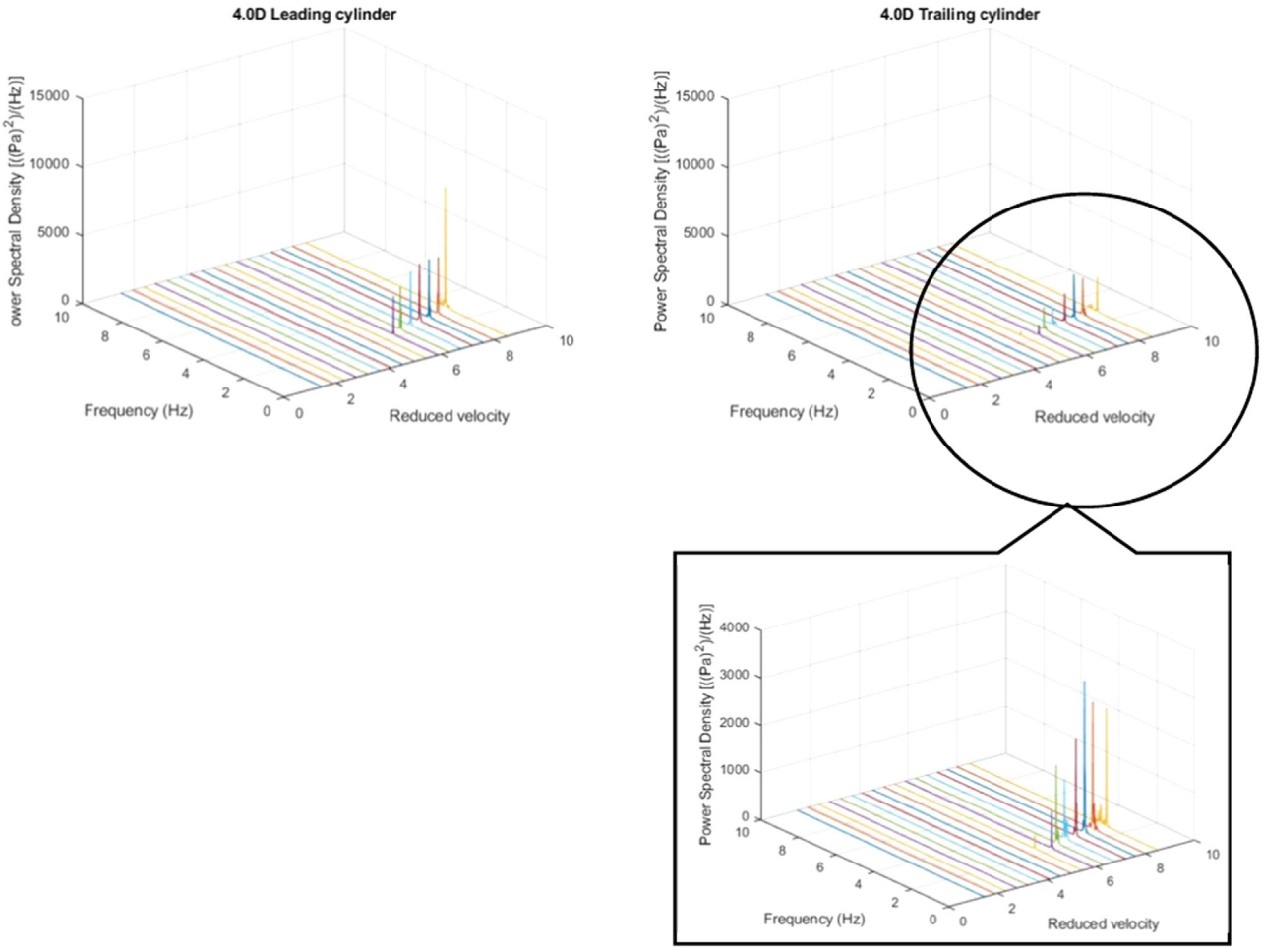

Fig. 11. PSD graphs of bare cylinders in tandem at 4.0*D*.

lation frequency in the lock-in region was close or equal to its natural frequency at $5.0 \leq V_r \leq 8.0$ (Fig. 7(b)). Meanwhile, the trailing cylinder's oscillation frequency increased monotonically and then locked on to the natural frequency up to the highest reduced velocity for all separation distances. According to Huera-Huarte and Gharib [23], Mysa et al. [55] and Song et al. [56], a trailing cylinder undergoing WIV would display an oscillation frequency that was closed to the natural frequency. Furthermore, the authors reported that the influence of various separation distances on frequency response was not clearly apparent, which corroborated the present study's findings.

To further evaluate the frequency response for $V_r > 9$, the behaviour of frequency response at $9 < V_r \leq 20$ by Korkischko and Meneghini [21] was adopted in this study. Based on the results, subsequent increases in frequency for the trailing cylinder at distances of 3.0 and 4.0 were reported, as depicted in Fig. 8. It becomes clear that the response of the trailing cylinder at the high reduced velocity was sustained by the WIV mechanism and the galloping phenomenon. According to Assi [26], the effect of vortex-induced vibration on the trailing cylinder's vibration weakened when the reduced velocity reached around 9.0 to 10.0. Following that, the wake-induced vibration dominated the cylinder's vibration.

4.3. Power spectral density (PSD)

The power spectral density analysis for the leading and trailing cylinders in the cross-flow direction with increasing flow velocity is presented in this section, along with selected typical time traces of cylinders' response at $V_r = 5.4$, 6.7, 7.6, and 8.5. Based on the 3-dimensional PSD graphs shown in Figs. 9, 11, and 13, the PSD's intensities of the CF responses were proportional to the selected amplitude responses shown in Figs. 10, 12, and 14. The PSD's responses in all figures show that all frequencies for leading and trailing cylinders at 3.5, 4.0 and 4.5*D* are narrow-banded with single peaks. According to the PSD graphs, the leading cylinder vibrated with a large amplitude due to the large PSD intensity generated during the oscillation. The peak PSD's response for the leading cylinder was higher than that of the trailing cylinder at all separation distances, 3.5, 4.0, and 4.5*D* for the higher reduced velocities, $V_r \geq 5.0$. The patterns of displacement and PSD were similar to those reported by Huera-Huarte and Bearman [22]. The PSD value increased as the amplitude of the oscillation increased. Nonetheless, the low peak of the trailing cylinder's PSD was consistent with its amplitude response. This observation depicted what happened to the trailing cylinder as the leading cylinder created the shielding effects [24]. The unprotected leading cylinder absorbed the energy from the moving water, causing it to vibrate stronger, yielding a high PSD value.

Based on the PSD's responses, the leading cylinder at 3.5*D* marked the highest PSD, around 11,600 Pa^2/Hz at $V_r = 8.5$ (Fig. 9), due to the high energy intensity produced by the intermittent reattachment and vortex shedding production during the bistable regime. This discontinuous change in the flow pattern could excite the energy intensity during oscillation. The discontinuous vortices formed in the gap between cylinders at 3.5*D* created a small

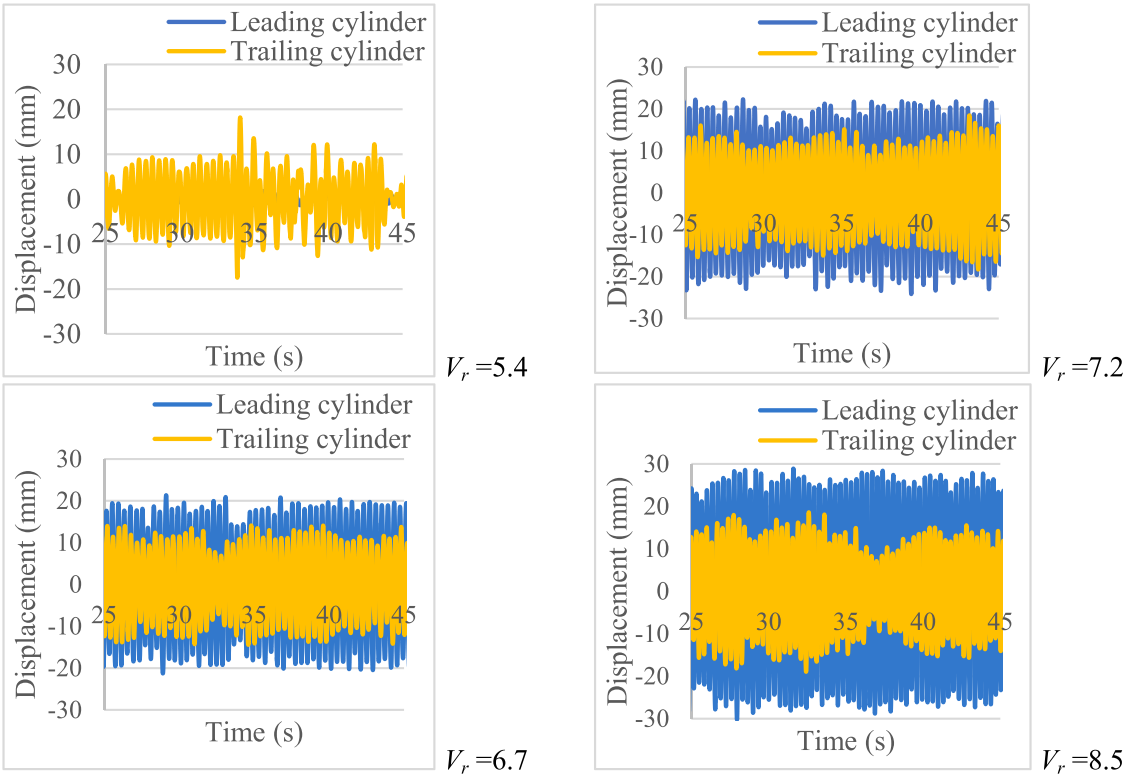

Fig. 12. The oscillation amplitudes of leading and trailing cylinders at 4.0*D*.

energy intensity at the trailing cylinder, which caused a low peak PSD at the trailing cylinder, around 2450 Pa^2/Hz at V_r = 8.5. The high energy intensity at the leading cylinder at V_r = 8.5 caused a larger oscillation (about 25 mm) in the leading cylinder's amplitude response (represented by the blue line in Fig. 10) than in the trailing cylinder's amplitude response (represented by the yellow line and is only around 10 mm). The time traces of the trailing cylinder in Fig. 10 also revealed that the trailing cylinder at 3.5*D* vibrated weaker than it was at 4.0 and 4.5*D* due to the low energy intensity.

Fig. 13 depicts that the PSD's response of the leading cylinder at 4.5*D* reached a maximum high value, around 9397 Pa^2/Hz at V_r = 8.5. As previously stated, the leading cylinder vibrated at a large amplitude due to the strong effect of wake-induced vibration with the existence of large vorticity behind the cylinder. Although the amplitude response in Fig. 6 shows that the leading cylinder at 4.5*D* was almost similar to the response at 3.5*D*, the PSD value of the leading cylinder at 4.5*D* was considerably smaller than the leading cylinder at 3.5*D*. This finding indicated that the leading cylinder experienced a critical condition at 3.5*D*.

The trailing cylinder vibrated with a small amplitude response at 3.5*D* due to the low energy intensity compared to 4.0 and 4.5*D*. The PSD's responses of the trailing cylinder at 4.0 and 4.5*D* appeared to be similar. However, based on the results, the PSD value of 4.5*D* was greater than that at 4.0*D*. The energy intensity for the trailing cylinder at 4.5*D* was enhanced by the large vortices emerging from the leading cylinder. It was about 3707 Pa^2/Hz for the trailing cylinder at V_r = 8.5, higher than the 2506 Pa^2/Hz at 4.0*D*.

If only the trailing cylinder could oscillate in the fluid-structure interaction between two rigid cylinders in a tandem arrangement, the trailing cylinder restores a large amplitude response at all separation distances [21]. However, different findings were obtained in the present study when both cylinders were allowed to move freely in the CF direction. The leading cylinder's amplitude grew larger than the trailing cylinder's amplitude, as the reduced velocity increased to the highest value. This situation was due to the leading cylinder's shielding effect on the trailing cylinder during the oscillation. Moreover, as Xu et al. [57] reported, the study on the rigid cylinder's response is significant because the rigid cylinder's results have been used extensively by the offshore industry to predict the VIV performance of a long flexible marine riser.

5. Conclusions and future works

In the present study, the VIV of the cylinders in the tandem arrangement was studied. In a water flume, tests were performed on a rigid cylinder oscillating in the wake of a leading cylinder, where both cylinders were free to oscillate transversely. The experiment arrangement remained constant all the time with varying *S/D* (*S/D* = 3.5, 4.0 and 4.5). Hence, the following conclusions can be made based on the experimental results:

(1) The tendency of increasing amplitude response was observed as the V_r increased. It was found that the lower branch of amplitude response was not indicated in the two cylinders' cases due to the effects of flow interference between the two tandem cylinders.
(2) The leading cylinder experienced a larger amplitude response than the trailing cylinder due to the shielding effect provided by the leading cylinder.
(3) The separation distance of 3.5*D* was determined to be the critical distance for the leading cylinder due to the bistable regime. Meanwhile, the trailing cylinder encountered a critical oscillation condition at 4.5*D*, with a significant lower oscillation amplitude and PSD values than the leading cylinder.

In our opinion, the findings necessitate further future research better to understand the effect of flow interference on the cylinders. Firstly, as explained in Section 4.1, the cylinders' vibration

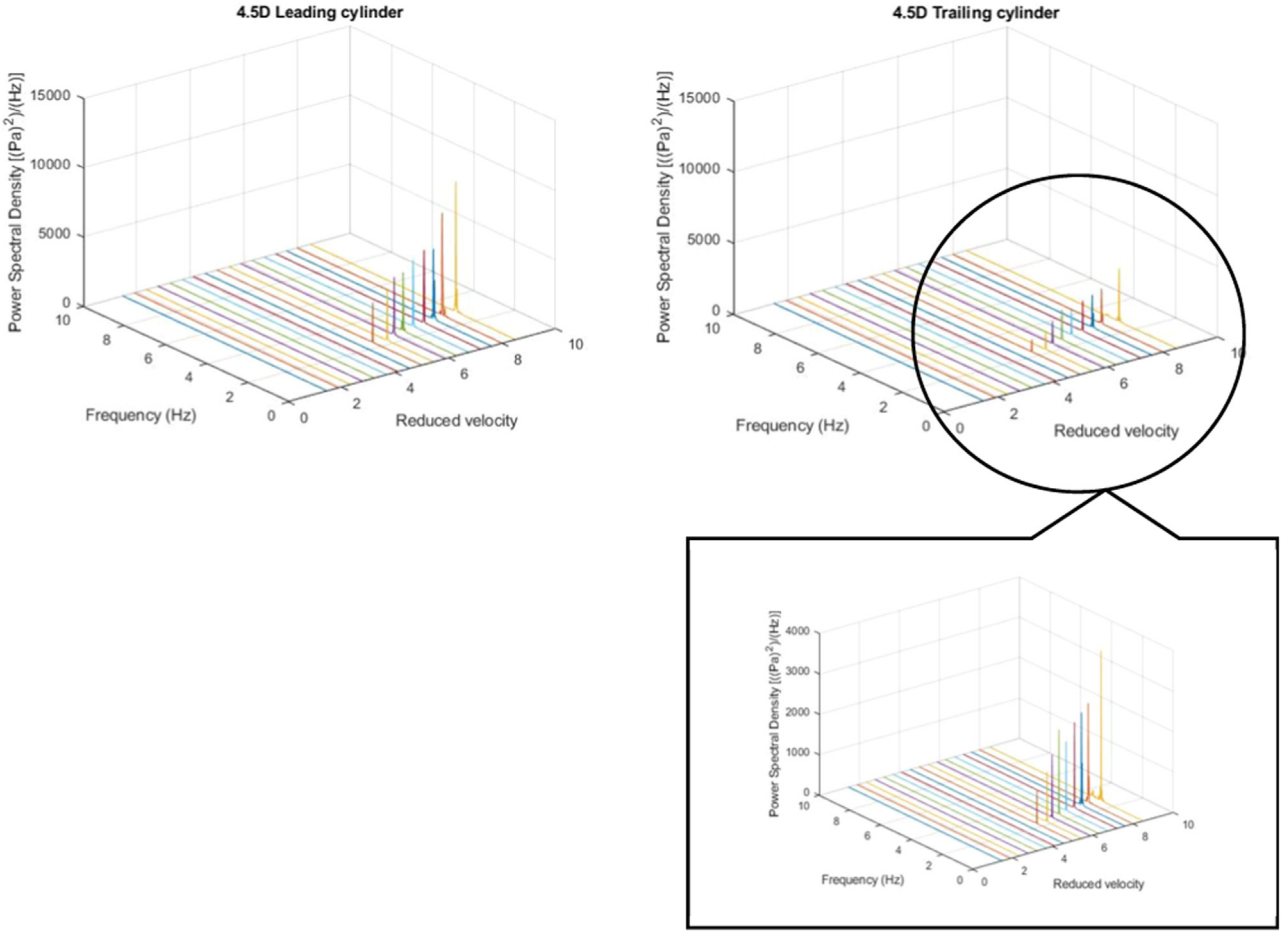

Fig. 13. PSD graphs of bare cylinders in tandem at 4.5*D*.

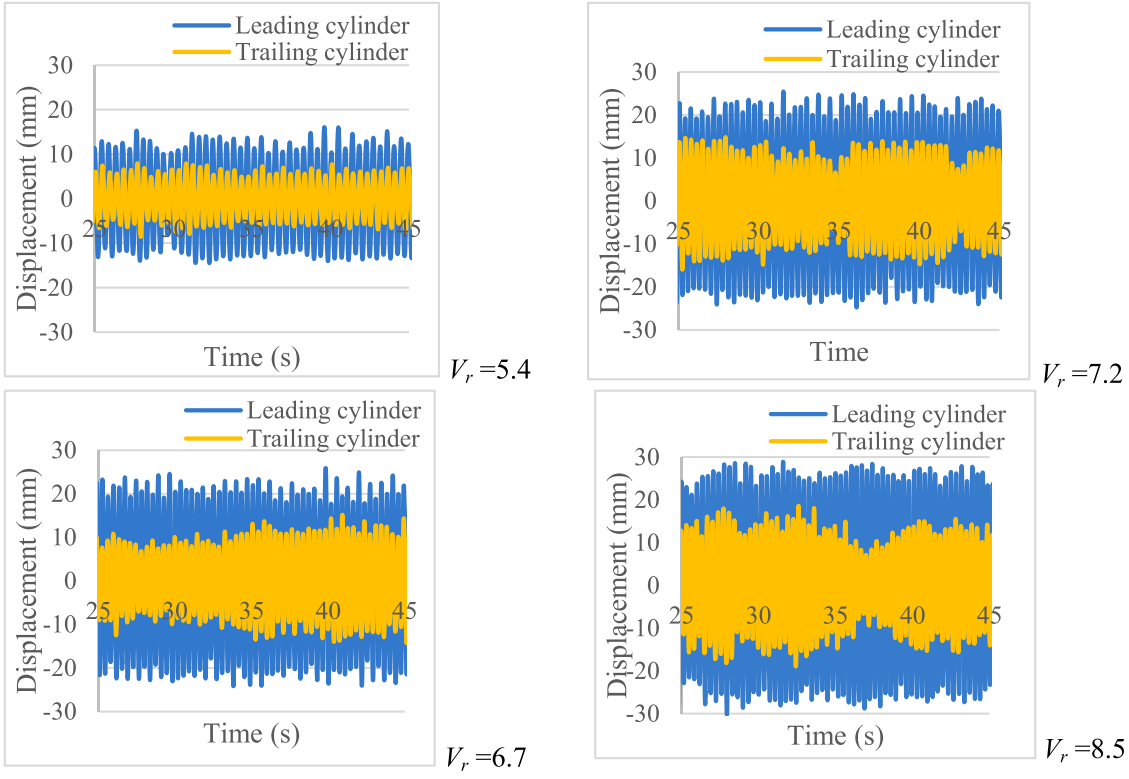

Fig. 14. The oscillation amplitudes of leading and trailing cylinders at 4.5*D*.

characteristics in a tandem arrangement should be investigated with a higher reduced velocity ($V_r > 10$). The wake-induced vibration phenomenon can be confirmed by providing the cylinders' responses at a higher reduced velocity. Secondly, an investigation of vortex-induced vibration of multiple cylinders should be expanded to include alternate cylinder arrangements, such as side-by-side and staggered, to identify critical arrangements further.

Funding

This work was financially supported by the Malaysian government under FRGS grants R.K130000.7843.5F297 and FRGS/1/2020/TK0/UTM/02/78.

Availability of data and material

Not applicable.

Code availability

Not applicable.

Ethics approval

Not applicable.

Consent to participate

Not applicable.

Consent for publication

All authors have approved the manuscript and agree with its submission to Journal of Ocean Engineering and Science.

Declaration of Competing Interest

The authors declare that they have no known competing financial interests or personal relationships that could have appeared to influence the work reported in this paper.

CRediT authorship contribution statement

Noor Idora Mohd Sukarnoor: Conceptualization, Methodology, Formal analysis, Investigation, Writing – original draft, Writing – review & editing. **Lee Kee Quen:** Conceptualization, Writing – review & editing, Funding acquisition, Supervision. **Aminudin Abu:** Writing – review & editing, Supervision. **Kang Hooi Siang:** Writing – review & editing, Supervision. **Noriyuki Kuwano:** Writing – review & editing, Supervision. **Safari Mat Desa:** Resources.

Acknowledgement

This work was financially supported by the Malaysian government under FRGS grants R.K130000.7843.5F297 and FRGS/1/2020/TK0/UTM/02/78. The authors also wish to acknowledge the National Hydraulic Research Institute of Malaysia (NAHRIM) for the facilities provided.

References

[1] P.R.F. Teixeira, P.P. Rechsteiner, E. Didier, J. Braz. Soc. Mech. Sci. Eng. 41 (8) (2019) 1–11, doi:10.1007/s40430-019-1835-3.
[2] X. Zhang, R. Gou, W. Yang, X. Chang, J. Braz. Soc. Mech. Sci. Eng. 40 (8) (2018) 1–12, doi:10.1007/s40430-018-1289-z.
[3] A. Farshidianfar, N. Dolatabadi, Acta Mech 224 (7) (2013) 1441–1456, doi:10.1007/s00707-013-0819-0.
[4] B. Fu, D. Wan, J. Ocean Eng. Sci. 2 (4) (2017) 268–278, doi:10.1016/j.joes.2017.09.001.
[5] S. Muddada, K. Hariharan, V.S. Sanapala, B.S.V. Patnaik, J. Ocean Eng. Sci. 6 (4) (2021) 389–399, doi:10.1016/j.joes.2021.04.002.
[6] P. Dey, A.K. Das, Eng. Sci. Technol. Int. J. 18 (4) (2015) 758–768, doi:10.1016/j.jestch.2015.05.007.
[7] W. Wang, Z. Mao, B. Song, P. Han, Phys. Fluids. 33 (3) (2021) 037127, doi:10.1063/5.0043185.
[8] M. Raiola, A. Ianiro, S. Discetti, Exp. Therm. Fluid Sci. 78 (2016) 354–369, doi:10.1016/j.expthermflusci.2016.06.003.
[9] H. Xue, K. Wang, W. Tang, Appl. Ocean Res. 52 (2015) 92–101, doi:10.1016/j.apor.2015.05.005.
[10] P. Kumar, S.K. Singh, J. Ocean Eng. Sci. 5 (2) (2020) 173–179, doi:10.1016/j.joes.2019.10.002.
[11] M.-.M. Liu, H.-.C. Wang, F.-.F. Shao, X. Jin, Tang G-Q, F. Yang, Appl. Ocean Res. 118 (2022) 102987, doi:10.1016/j.apor.2021.102987.
[12] D. Sumner, J. Fluids Struct. 26 (6) (2010) 849–899, doi:10.1016/j.jfluidstructs.2010.07.001.
[13] F.J. Huera-Huarte, Z.A. Bangash, L.M. González, J. Fluids Struct. 66 (2016) 571–588, doi:10.1016/j.jfluidstructs.2016.07.019.
[14] M.M. Alam, M. Elhimer, L.J. Wang, D. Lo Jacono, C.W. Wong, Exp. Fluids. 59 (3) (2018) 1–17, doi:10.1007/s00348-018-2501-8.
[15] H. Zhu, C. Zhang, W. Liu, Phys. Fluids. 31 (7) (2019) 073606, doi:10.1063/1.5106407.
[16] X. Fan, Z. Wang, Y. Wang, W. Tan, Int. J. Mech. Sci. 192 (2021) 106132, doi:10.1016/j.ijmecsci.2020.106132.
[17] M.M. Zdravkovich, D.L. Pridden, I, J. Wind Eng. Ind. Aerodyn. 2 (3) (1977) 255–270 https://doi.org/10.1016/0167-6105(77)90026-5.
[18] T. Igarashi, Bull. JSME 24 (188) (1981) 323–331, doi:10.1299/jsme1958.24.323.
[19] G.R.S. Assi, J.R. Meneghini, J.A.P. Aranha, P.W. Bearman, E. Casaprima, J. Fluids Struct. 22 (6) (2006) 819–827, doi:10.1016/j.jfluidstructs.2006.04.013.
[20] S. Kim, M.M. Alam, H. Sakamoto, Y. Zhou, J. Wind Eng. Ind. Aerodyn. 97 (2009) 304–311, doi:10.1016/j.jweia.2009.07.004.
[21] I. Korkischko, J.R. Meneghini, J. Fluids Struct. 26 (4) (2010) 611–625, doi:10.1016/j.jfluidstructs.2010.03.001.
[22] F.J. Huera-Huarte, P.W. Bearman, J. Fluids Struct. 27 (2) (2011) 193–211, doi:10.1016/j.jfluidstructs.2010.11.004.
[23] F.J. Huera-Huarte, M. Gharib, J. Fluids Struct. 27 (5) (2011) 824–828, doi:10.1016/j.jfluidstructs.2011.02.006.
[24] S. Huang, A. Sworn, Appl. Ocean Res. 43 (2013) 21–26, doi:10.1016/j.apor.2013.06.001.
[25] K. Lin, D. Fan, J. Wang, Ocean Eng 209 (2020) 107520, doi:10.1016/j.oceaneng.2020.107520.
[26] G.R.S. Assi, J. Fluids Struct. 50 (2014) 329–339, doi:10.1016/j.jfluidstructs.2014.07.001.
[27] W. Xu, Y. Ma, A. Cheng, H. Yuan, Int. J. Mech. Sci. 135 (2018) 261–278, doi:10.1016/j.ijmecsci.2017.11.027.
[28] A. Bakhtiari, M. Zeinoddini, H. Ashrafipour, V. Tamimi, M.M.A. Harandi, P. Jadidi, Ocean Eng 216 (2020) 108093, doi:10.1016/j.oceaneng.2020.108093.
[29] A. Bokaian, F. Geoola, J. Fluids Mech. 146 (1984) 383–415, doi:10.1017/S0022112084001920.
[30] X. Fan, K. Guo, Z. Jia, Y. Wang, W. Tan, J. Wind Eng. Ind. Aerodyn. 199 (2020) 104136, doi:10.1016/j.jweia.2020.104136.
[31] J.S. Wang, D.X. Fan, K. Lin, J. Hydrodyn. 32 (3) (2020) 415–440, doi:10.1007/s42241-020-0032-2.
[32] M. Zhao, J.M. Murphy, K. Kwok, J. Fluids Eng. 138 (2) (2016) 021102, doi:10.1115/1.4031257.
[33] R.C. Mysa, A. Kaboudian, R.K. Jaiman, J. Fluids Struct. 61 (2016) 76–98, doi:10.1016/j.jfluidstructs.2015.11.004.
[34] S.V. Singh, P. Mitra, P. Kumar, J. Ocean Eng. Sci. 6 (3) (2021) 248–256, doi:10.1016/j.joes.2021.01.001.
[35] B. Sharman, F.S. Lien, L. Davidson, C. Norberg, Int. J. Numer. Methods Fluids. 47 (5) (2005) 423–447, doi:10.1002/fld.812.
[36] N.M.R. Shaharuddin, I.Z.M. Darus, Acta Mech 226 (11) (2015) 3795–3806, doi:10.1007/s00707-015-1438-8.
[37] G.R. Franzini, A.L.C. Fujarra, J.R. Meneghini, I. Korkischko, R. Franciss, J. Fluids Struct. 25 (4) (2009) 742–750, doi:10.1016/j.jfluidstructs.2009.01.003.
[38] Khalak A, C.H.K. Williamson, J. Fluids Struct. 13 (7) (1999) 813–851, doi:10.1006/jfls.1999.0236.
[39] F.A.C. Martins, J.P.J. Avila, Int. J. Mech. Sci. 156 (2019) 235–249, doi:10.1016/j.ijmecsci.2019.03.024.
[40] A. Jain, Y. Modarres-Sadeghi, J. Fluids Struct. 43 (2013) 28–40, doi:10.1016/j.jfluidstructs.2013.08.005.
[41] Z. Hu, J. Wang, Y. Sun, Ocean Eng. 209 (2020) 107501, doi:10.1016/j.oceaneng.2020.107501.
[42] R.D. Blevins, Flow-induced vibrations, Second Ed., Van Nostrand Reinhold, New York, 1990.
[43] R.N. Govardhan, C.H.K. Williamson, J. Fluids Mech. 561 (2006) 147–180, doi:10.1017/S0022112006000310.
[44] M.A.A. Rahman, K.P. Thiagarajan, Int. J. Automot. Mech. Eng. 11 (2015) 2515–2530 https://doi.org/10.15282/ijame.11.2015.31.0212.
[45] M.A.A. Rahman, 2015.
[46] A. Bakhtiari, M. Zeinoddini, H. Ashrafipour, V. Tamimi, Appl. Ocean Res. 105 (2020) 102406, doi:10.1016/j.apor.2020.102406.
[47] G.V. Papaioannou, D.K.P. Yue, M.S. Triantafyllou, G.E. Karniadakis, J. Fluids Struct. 24 (6) (2008) 833–854, doi:10.1016/j.jfluidstructs.2007.11.006.

[48] L. Ding, M.M. Bernitsas, E.S. Kim, Ocean Eng. 72 (2013) 429–440, doi:10.1016/j.oceaneng.2013.06.005.
[49] M.M. Zdravkovich, J. Fluids Struct. 1 (2) (1987) 239–261 https://doi.org/10.1016/S0889-9746(87)90355-0.
[50] M. Elhimer, G. Harran, Y. Hoarau, S. Cazin, M. Marchal, M. Braza, J. Fluids Struct. 60 (2016) 62–79, doi:10.1016/j.jfluidstructs.2015.10.008.
[51] M.M. Zdravkovich, J. Sound Vib. 101 (4) (1985) 511–521 https://doi.org/10.1016/S0022-460X(85)80068-7.
[52] S. Ishigai, E. Nishikawa, K. Nishimura, K. Cho, Bull. JSME 15 (86) (1972) 949–956, doi:10.1299/jsme1958.15.949.
[53] M. Lou, Z. Chen, P. Chen, J. Nat. Gas Sci. Eng. 35 (2016) 736–752, doi:10.1016/j.jngse.2016.09.012.
[54] T. Zheng, S.K. Tang, B. Fei, Trans. Can. Soc. Mech. Eng. 33 (3) (2009) 349–360, doi:10.1139/tcsme-2009-0025.
[55] R.C. Mysa, Y.Z. Law, R.K. Jaiman, J. Fluids Struct. 75 (2017) 27–44, doi:10.1016/j.jfluidstructs.2017.08.001.
[56] H. Song, W. Huang, S. Chang, Ocean Eng. 195 (2020) 106746, doi:10.1016/j.oceaneng.2019.106746.
[57] J. Xu, M. He, N. Bose, Ocean Eng. 36 (6) (2009) 456–467, doi:10.1016/j.oceaneng.2009.01.010.